2024 European Control Conference (ECC)
June 25-28, 2024. Stockholm, Sweden

Hierarchical distributed scenario-based model predictive control of interconnected microgrids*

T. Alissa Schenck[1] and Christian A. Hans[2]

Abstract— **Microgrids are autonomous clusters of generators, storage units and loads. Special requirements arise in interconnected operation: control schemes that do not require individual microgrids to disclose information about their internal structure and operating objectives are preferred for privacy reasons. Moreover, a safe and economically meaningful operation shall be achieved in presence of uncertain load and weather-dependent availability of renewable infeed. In this paper, we propose a hierarchical distributed model predictive control approach that satisfies these requirements. Specifically, we demonstrate that costs and safety of supply can be improved through a scenario-based stochastic control scheme. In a numerical case study, our approach is compared to a certainty equivalence and a prescient scheme. The results illustrate good performance as well as sufficiently fast convergence.**

I. Introduction

Climate change is one of the major challenges of the 21st century. Renewable energy sources (RESs) play a central role in tackling this challenge. As infeed of RESs increases, new questions arise: how to ensure a reliable operation in presence of uncertain RESs and how to keep the complexity manageable despite a large number small-scale RESs?

Microgrids (MGs) have emerged as a promising approach to answer these questions. An MG clusters a collection of loads and distributed units [1], such as storage units, RESs and conventional generators. Internally, it is controlled in a way that makes it appear as a single subsystem [2] to the outside world which acts as a load or a generator [1] when connected to a utility grid. Compared to islanded operation, trading energy between interconnected MGs allows to further increase infeed of RESs with different generation patterns.

Operation control, also referred to as energy management, aims to provide power setpoints to the units and thereby control the energy of storages. For this task, model predictive control (MPC) has been widely employed. Here, optimization problems are solved to find control actions that minimize an objective subject to constrains which model the system behavior and account for limits. Decisions have to be made in presence of uncertain load and renewable infeed. In state-of-the-art approaches, nominal forecasts are often assumed to be certain which holds the risk of constraint violations in presence of prediction errors. Stochastic approaches, that employ forecast probability distributions, on the other hand, allow to increase robustness and performance [3].

*Note that this work is based on the master thesis "Stochastic model predictive control of interconnected microgrids" by T. Alissa Schenck.

[1]T. Alissa Schenck received a master's degree from Technische Universität Berlin, Germany, ta-schenck@posteo.de.

[2]Christian A. Hans is with the Automation and Sensorics in Networked Systems Group, University of Kassel, Germany, hans@uni-kassel.de.

Stochastic MPC of MGs was actively explored in recent years. In [4], a scenario-based method for the optimal operation of a single grid-connected MG was proposed. Kou et al. consider a similar setup in [5]. In [6], a scenario-based approach consisting of optimal generation scheduling and MPC is presented. The authors of [7] propose a scenario-based approach that employs heuristics for optimal control. Heymann et al. model the demand dynamics with stochastic differential equation and solve a management problem [8]. Only few have studied stochastic control of networks of interconnected MGs, probably because such problems can be hard to decompose and stochastic mixed-integer problems (MIPs) often do not scale well. To our knowledge, only in [9], a multi-MG system with uncertain RESs and load as well as power exchange between MGs is considered. However, the approach relies on day-ahead scheduling which can be inflexible in grid with high share of uncertain renewable energy sources.

In this work, we employ a hierarchical distributed MPC approach [10] in a setting where scenario-based stochastic local problems along the lines of [11] are considered. In this context, the following contributions are made. (i) Uncertainties in renewable generation and loads are handled by inclusion of forecast probability distributions. In the overall MPC scheme, we assume that fluctuations are covered within each MG and power flow over the AC grid is certain. (ii) We solve the MPC problem through a distributed algorithm that is based on the widely employed alternating direction method of multipliers (ADMM) (see, e.g., [10], [12], [13]). Control actions are found by alternately solving local stochastic optimization problems at individual MGs and a certainty equivalence optimization problem at a central coordinator that takes care of the power flow between the MGs. The algorithm allows to respect the privacy and independence of individual MGs. In addition, the computational complexity scales well with the number of MGs such that solve times remain manageable. (iii) In a comprehensive case study, the stochastic approach is thoroughly compared with the certainty equivalence approach from [10] and a prescient MPC. Several closed-loop performance metrics as well as solve times and number of iterations are assessed. The results highlight the increased security of the novel approach compared to certainty equivalence MPC.

The remainder of this paper is structured as follows. In Section II, the plant model and the model of the uncertain forecast are introduced. In Section III, a problem formulation is provided and in Section IV, a distributed solution proposed. Finally, in Section V simulation results are discussed.

TABLE I
VARIABLES OF MG i BY UNIT TYPE

	Variable	Type	Symbol
Convent.	Setpoint	Control input	$u_{t,i} \in \mathbb{R}_{\geq 0}^{T_i}$
	On/off switch	Control input	$\delta_{t,i} \in \mathbb{B}^{T_i}$
	Power	Auxiliary	$p_{t,i} \in \mathbb{R}_{\geq 0}^{T_i}$
Storage	Setpoint	Control input	$u_{s,i} \in \mathbb{R}^{S_i}$
	Energy	State	$x_i \in \mathbb{R}_{\geq 0}^{S_i}$
	Power	Auxiliary	$p_{s,i} \in \mathbb{R}^{S_i}$
	Slack var.	Auxiliary	$\sigma_i \in \mathbb{R}_{\geq 0}^{S_i}$
RES	Setpoint	Control input	$u_{r,i} \in \mathbb{R}_{\geq 0}^{R_i}$
	Weather-dependent available power	Uncertain input	$w_{r,i} \in \mathbb{R}_{\geq 0}^{R_i}$
	Power	Auxiliary	$p_{r,i} \in \mathbb{R}_{\geq 0}^{R_i}$
	Boolean var. for min-operator	Auxiliary	$\delta_{r,i} \in \mathbb{B}^{R_i}$
Load	Power	Uncertain input	$w_{d,i} \in \mathbb{R}_{\leq 0}^{D_i}$
Grid	PCC Power	Auxiliary	$p_{g,i} \in \mathbb{R}$
	Power sharing var.	Auxiliary	$\rho_i \in \mathbb{R}$

A. Notation

The set of positive integers is $\mathbb{N}$ and the set of nonnegative integers $\mathbb{N}_0$. The set of Boolean variables is $\mathbb{B} = \{1, 0\}$. The set $\{x | x \in \mathbb{N}_0 \wedge a \leq x \leq b\}$ is shortly referred to as $\mathbb{N}_{[a,b]}$. The set of real numbers is $\mathbb{R}$, the set of negative real numbers $\mathbb{R}_{<0}$ and the set of positive real numbers $\mathbb{R}_{>0}$. Likewise, $\mathbb{R}_{\leq 0}$ denotes nonpositive and $\mathbb{R}_{\geq 0}$ nonnegative real numbers.

Let $\mathbf{1}_n$ be the n-dimensional column vector of all ones. Moreover, $\mathbf{0}_{m \times n}$ is the $m \times n$ matrix of all zeros and $\mathbf{I}_n$ the $n \times n$ identity matrix. Consider a vector $a = [a_1 \ \cdots \ a_n]^\top$. Then $\mathrm{diag}(a)$ is a diagonal matrix with entries a_i, $i \in \mathbb{N}_{[1,n]}$. Finally, $\|a\|_2$ is the Euclidean norm of vector a.

II. MODEL

In what follows, the model of a network of AC MGs (see, e.g., Figure 1) is derived. Moreover, the representation of uncertain forecasts in the form of scenario trees is discussed.

A. MG model variables

Consider $I \in \mathbb{N}$ MGs which are uniquely indexed by elements of the set $\mathbb{I} = \mathbb{N}_{[1,I]}$. Each MG $i \in \mathbb{I}$ is composed of $T_i \in \mathbb{N}$ conventional units, $S_i \in \mathbb{N}$ storage units, $R_i \in \mathbb{N}$ RESs and $D_i \in \mathbb{N}$ loads. The variables associated with MG i are collected in Table I. For the units, active sign convention is used, i.e., positive values indicate that power is provided, negative values that it is consumed. For MG i, the power setpoints of all units are collected in $u_i = [u_{t,i}^\top \ u_{s,i}^\top \ u_{r,i}^\top]^\top$ and the control inputs combined in $v_i = [u_i^\top \ \delta_{t,i}^\top]^\top$. The power values are collected in $p_i = [p_{t,i}^\top \ p_{s,i}^\top \ p_{r,i}^\top]^\top$ which is used to form $q_i = [p_i^\top \ \delta_{r,i}^\top \ \sigma_i^\top \ \rho_i]^\top$. The state x_i represents the energy that is contained in the storage units. Finally, $w_i = [w_{r,i}^\top \ w_{d,i}^\top]^\top$ is the vector of uncertain inputs.

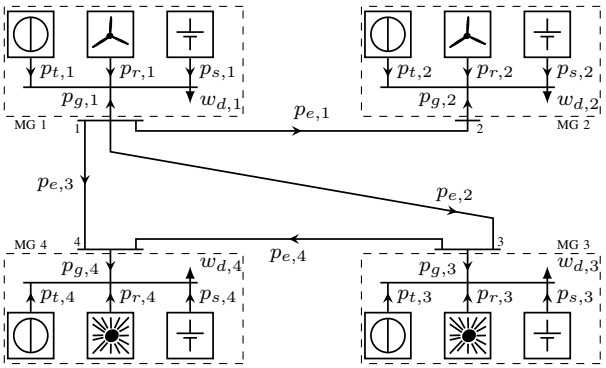

Fig. 1. Topology of four interconnected AC MGs from [10].

B. Uncertainty model

The forecasts of uncertain load and weather-dependent available renewable infeed are modeled using scenario trees. This section provides a brief introduction on their generation and structure. Note that it is strongly motivated by [3].

1) From forecast scenarios to scenario trees: Consider a finite number of independent equiprobable forecast scenarios proceeding into the future for J prediction steps. For a large number of scenarios, the underlying probability distribution is accurately approximated. Since a large number of scenarios leads to complex optimization problems, more compact representations of probability distributions, such as scenario trees, are desirable. In this paper, forecast scenarios of available wind power are derived using autoregressive integrated moving average (ARIMA) models. The available photovoltaic power and load demand forecast scenarios are generated using seasonal ARIMA models. On these scenarios, forward selection [14] is applied to obtain scenario-trees.

2) Scenario tree structure: Scenario trees are collections of $M_i \in \mathbb{N}$ nodes which are partitioned into $J \in \mathbb{N}$ stages, i.e., prediction steps $j \in \mathbb{N}_{[0,J]}$. Let us collect the unique indices of all nodes in $\mathbb{M}_i = \mathbb{N}_{[0,M_i-1]}$. The $\mathrm{stage}_i(m)$ operator provides the stage of node $m \in \mathbb{M}_i$. Likewise, $\mathrm{nodes}_i(j)$ provides the set of nodes associated with stage j. We refer to the node $m = 0$ at stage $j = 0$ as the root node and the nodes at stage $j = J$ as leaf nodes. The set of all non-root nodes is $\mathbb{L}_i = \mathbb{M}_i \setminus \{0\}$. Each node $m \in \mathrm{nodes}_i(j)$ at stage $j \in \mathbb{N}_{[0,J-1]}$ is connected to a set of child nodes at stage $j+1$ which are accessible via $\mathrm{child}_i(m)$. Vice versa, all nodes $m \in \mathrm{nodes}_i(j)$ at stage $j \in \mathbb{N}_{[1,J]}$ are reachable from one unique ancestor node at stage $j-1$, denoted $\mathrm{anc}_i(m)$. The probability to visit node m is $\pi^{(m)} \in (0, 1] \subset \mathbb{R}$. By construction of the tree, we have that

$$\sum_{m \in \mathrm{nodes}_i(j)} \pi^{(m)} = 1 \qquad \forall j \in \mathbb{N}_{[0,J]} \quad \text{and} \tag{1a}$$

$$\sum_{m_+ \in \mathrm{child}_i(m)} \pi^{(m_+)} = \pi^{(m)} \quad \forall m \in \mathbb{M}_i \setminus \mathrm{nodes}_i(J). \tag{1b}$$

Each node $m \in \mathbb{M}_i$ is associated with a vector of states $x_i^{(m)}$ (see Figure 2). Moreover, $v_i^{(m)}$ represents the control inputs, $w_i^{(m)}$ the uncertain inputs and $q_i^{(m)}$ the auxiliary variables associated with node $m \in \mathbb{L}_i$.

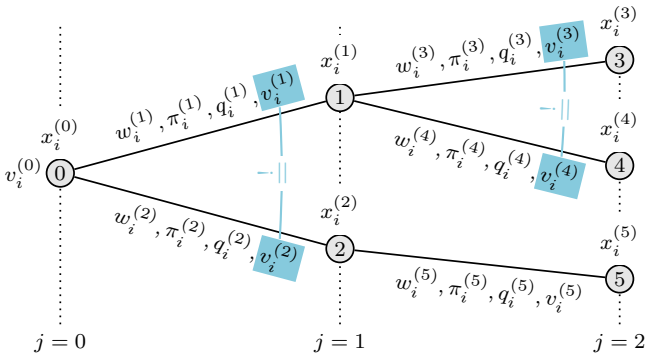

Fig. 2. Scenario tree based on [11] with nonanticipativity constraints.

3) Nonanticipativity: In the upcoming stochastic optimization problems, we aim to make control decisions $v_i^{(m)}$ at each node $m \in \mathbb{L}_i$. In this context, it is important to move causally in time: When making control decisions, we do not know exactly which uncertain input will occur. We only know possible outcomes and associated probabilities. Thus, we need make *one* decision for *all* uncertain inputs that originate from the same ancestor. This must be accounted for, e.g., by the equality constraint

$$v_i^{(m)} = v_i^{(n)} \quad \forall n \in \mathrm{child}_i(\mathrm{anc}_i(m)). \tag{2}$$

In Figure 2, this so-called nonanticipativity constraint (see, e.g., [15]–[17]) is illustrated in light blue. Here, at stage $j = 1$, we can only make one control decision $v_i^{(1)} = v_i^{(2)}$ for the possible uncertain inputs $w_i^{(1)}$ and $w_i^{(2)}$. At stage $j = 2$, when finding control actions for nodes 3 and 4, we can only use the information that is available up to node 1, i.e., we consider the case associated with uncertain input $w_i^{(1)}$. Here, we need to make one decision $v_i^{(3)} = v_i^{(4)}$ for possible uncertain inputs $w_i^{(3)}$ and $w_i^{(4)}$. Since node 5 is a singleton, no restrictions of the form (2) apply.

Remark 1: In problem formulations, nonanticipativity can be included in different ways. One possibility is replacing $v_i^{(n)}$ by $v_i^{(m)}$ for all $n \in \mathrm{child}_i(\mathrm{anc}_i(m))$ when formulating the problems. Another way is to include (2) as a regular constraint. In this case, the pre-solve stage in off-the-shelf solvers, would often perform aforementioned replacement internally. Either way, (2) reduces the complexity of associated problems since less decision variables must be considered. •

C. Single microgrid model

In what follows, a model of a single AC MG is derived. It is based on [11] and includes RESs, storage and conventional units as well as a point of common coupling (PCC).

1) RESs: The forecasts of power and setpoint must lie within the bounds $p_{r,i}^{\min} \in \mathbb{R}_{\geq 0}^{R_i}$ and $p_{r,i}^{\max} \in \mathbb{R}_{>0}^{R_i}$, i.e.,

$$p_{r,i}^{\min} \leq u_{r,i}^{(m)} \leq p_{r,i}^{\max}, \tag{3a}$$
$$p_{r,i}^{\min} \leq p_{r,i}^{(m)} \leq p_{r,i}^{\max}, \tag{3b}$$

for all $m \in \mathbb{L}_i$ [11]. Additionally, the power of each RES can be limited by its setpoint. The limit comes to bear if the weather-dependent available renewable power exceeds the setpoint. If it lies below the setpoint, then the power follows the available infeed. Using the element-wise min operator allows to describe this for all $m \in \mathbb{L}_i$ by [11]

$$p_{r,i}^{(m)} = \min(u_{r,i}^{(m)}, w_{r,i}^{(m)}). \tag{4}$$

Note that (4) can be easily transformed into a set of affine constraints using the auxiliary decision variable $\delta_{r,i}^{(m)}$ (see, e.g., [3, Lemma 3.3.6]) which makes it appropriate for MIPs.

2) Storage units: The forecasts of setpoints and power are limited by $p_{s,i}^{\min} \in \mathbb{R}_{<0}^{S_i}$ and $p_{s,i}^{\max} \in \mathbb{R}_{>0}^{S_i}$, i.e.,

$$p_{s,i}^{\min} \leq u_{s,i}^{(m)} \leq p_{s,i}^{\max}, \tag{5a}$$
$$p_{s,i}^{\min} \leq p_{s,i}^{(m)} \leq p_{s,i}^{\max}, \tag{5b}$$

for all $m \in \mathbb{L}_i$ [11]. Moreover, the storage units exhibit dynamics which can be forecast for all $m \in \mathbb{L}_i$ via

$$x_i^{(m)} = x_i^{(m_-)} - T_s p_{s,i}^{(m)}, \tag{6}$$

with $m_- \in \mathrm{anc}_i(m)$ [11]. Here, $x_i^{(0)} = x_i(k)$ is the measured state at the current discrete time instant $k \in \mathbb{N}_0$. It is desired to keep $x_i^{(m)}$ above $x_i^{\min} \in \mathbb{R}_{\geq 0}^{S_i}$ and below $x_i^{\max} \in \mathbb{R}_{>0}^{S_i}$. To ensure feasibility, $\sigma_i^{(m)} \in \mathbb{R}_{\geq 0}^{S_i}$ is used to form the soft constraints

$$x_i^{\min} - \sigma_i^{(m)} \leq x_i^{(m)} \leq x_i^{\max} + \sigma_i^{(m)} \tag{7}$$

for all $m \in \mathbb{L}_i$ which are completed by adding a penalty on nonzero values of $\sigma_i^{(m)}$ to the objective in Section III-A.

3) Conventional units: The forecasts of power and setpoints must lie within $p_{t,i}^{\min} \in \mathbb{R}_{>0}^{T_i}$ and $p_{t,i}^{\max} \in \mathbb{R}_{>0}^{T_i}$ for enabled units. With the Boolean input $\delta_{t,i}^{(m)}$ that indicates if units are enabled or disabled, this can be formulated as [11]

$$\mathrm{diag}\left(p_{t,i}^{\min}\right) \delta_{t,i}^{(m)} \leq u_{t,i}^{(m)} \leq \mathrm{diag}\left(p_{t,i}^{\max}\right) \delta_{t,i}^{(m)}, \tag{8a}$$
$$\mathrm{diag}\left(p_{t,i}^{\min}\right) \delta_{t,i}^{(m)} \leq p_{t,i}^{(m)} \leq \mathrm{diag}\left(p_{t,i}^{\max}\right) \delta_{t,i}^{(m)}. \tag{8b}$$

4) Power sharing between grid-forming units: We assume that grid-forming storage and conventional units change their power in presence of fluctuations in a given proportional manner. This is typically achieved via suitable low-level control schemes (see, e.g., [18]) and can be modeled by [3]

$$K_{t,i}(p_{t,i}^{(m)} - u_{t,i}^{(m)}) = \rho_i^{(m)} \delta_{t,i}^{(m)}, \tag{9a}$$
$$K_{s,i}(p_{s,i}^{(m)} - u_{s,i}^{(m)}) = \rho_i^{(m)} \mathbf{1}_{S_i}, \tag{9b}$$

for all $m \in \mathbb{L}_i$ with the auxiliary decision variable $\rho_i^{(m)}$ and the droop coefficient matrices

$$K_{t,i} = \mathrm{diag}([1/\chi_{i,1} \quad \cdots \quad 1/\chi_{i,T_i}]^\top),$$
$$K_{s,i} = \mathrm{diag}([1/\chi_{i,(T_i+1)} \quad \cdots \quad 1/\chi_{i,(T_i+S_i)}]^\top).$$

Here, the design parameters $\chi_{i,l} \in \mathbb{R}_{>0}$, $l \in \mathbb{N}_{[1,T_i+S_i]}$ can be chosen for example according to the units' nominal power.

The term $\rho_i^{(m)} \delta_{t,i}^{(m)}$ in (9a) models that only enabled units can participate in power sharing. It can be easily transformed into a set of affine constraints (see, e.g., [3, Lemma 3.3.5]) which renders it appropriate for mixed-integer formulations.

5) PCC power: We assume that the low-level control schemes keep the power at the PCC at a desired value $p_{g,i}(j)$ in presence of uncertain demand and renewable infeed. Thus, all fluctuations are covered inside each MG i and power exchange over the utility grid is *not* affected by uncertainties, i.e., it is certain. In the model, this is captured by only considering *one* predicted PCC power value $p_{g,i}(j)$ which is identical for all nodes at stage $j \in \mathbb{N}_{[1,J]}$. This power is limited by $p_{g,i}^{\min} \in \mathbb{R}_{\leq 0}$ and $p_{g,i}^{\max} \in \mathbb{R}_{\geq 0}$, i.e.,

$$p_{g,i}^{\min} \leq p_{g,i}(j) \leq p_g^{\max}. \tag{10}$$

6) Local power balance: Within each MG $i \in \mathbb{I}$, a local power balance holds. For all $m \in \mathbb{L}_i$, it is modeled by

$$0 = \mathbf{1}_{R_i}^\top p_{r,i}^{(m)} + \mathbf{1}_{T_i}^\top p_{t,i}^{(m)} + \mathbf{1}_{S_i}^\top p_{s,i}^{(m)} + \mathbf{1}_{D_i}^\top w_{d,i}^{(m)} + p_{g,i}(\mathrm{stage}_i(m)). \tag{11}$$

D. Grid model

Let us collect the PCC power forecast $p_{g,i}(j)$ of all MGs at stage $j \in \mathbb{N}_{[1,J]}$ in $p_g(j) = [p_{g,1}(j) \ \cdots \ p_{g,I}(j)]^\top$. Negative values of $p_{g,i}(j)$ indicate that MG i injects power into the grid, whereas a positive values indicates a consumption of power. Let us further collect the power flow over $E \in \mathbb{N}$ transmission lines in $p_e(k) = [p_{e,1}(k) \ \cdots \ p_{e,E}(k)]^\top$. Assuming inductive short to medium length power lines allows us to employ the DC power flow approximations for AC grids [19]. Motivated by [10], we describe the power flow over the lines by

$$p_e(j) = \tilde{F} \cdot p_g(j). \tag{12a}$$

Moreover, a global power equilibrium of the form

$$0 = \mathbf{1}_I^\top p_g(j) \tag{12b}$$

must hold. The power that can be transmitted via the grid is limited by $p_e^{\min} \in \mathbb{R}_{<0}^E$ and $p_e^{\max} \in \mathbb{R}_{>0}^E$, i.e.,

$$p_e^{\min} \leq p_e(j) \leq p_e^{\max}. \tag{12c}$$

III. Problem formulation

Based on the model from the previous chapter, we can now formulate MPC problems for the operation of interconnected MGs. We start by discussing the operation costs.

A. Costs of individual MGs

In what follows, we define the units' costs for all nodes $m \in \mathbb{L}_i$ in the scenario trees of each MG $i \in \mathbb{I}$.

1) RESs: The desire for high renewable infeed is considered by penalizing deviations from the rated power $p_{r,i}^{\max}$. With weight $c_{r,i} \in \mathbb{R}_{>0}^{R_i}$ the cost is formulated as [10]

$$\ell_{r,i}^{(m)} = \| \operatorname{diag}(c_{r,i})(p_{r,i}^{\max} - p_{r,i}^{(m)}) \|_2^2. \tag{13}$$

2) Storage units: The costs of the storage units are

$$\ell_{s,i}^{(m)} = \| \operatorname{diag}(c_{s,i}) p_{s,i}^{(m)} \|_2^2 + \| \operatorname{diag}(c_{\sigma,i}) \sigma_i^{(m)} \|_2^2 \tag{14}$$

with $c_{s,i} \in \mathbb{R}_{>0}^{S_i}$ and $c_{\sigma,i} \in \mathbb{R}_{>0}^{S_i}$. The first term reflects conversion losses, the second term is a penalty for nonzero values of $\sigma_i^{(m)}$, i.e., energy values above $x_i^{\max}$ or below $x_i^{\min}$ (see Section II-C.2).

3) Conventional generators: Following [20], the operating costs of the conventional units are modeled using a quadratic function. With $c_{t,i}$, $c'_{t,i}$, $c''_{t,i} \in \mathbb{R}_{>0}^{T_i}$, it reads

$$\ell_{t,i}^{(m)} = c_{t,i}^\top \delta_{t,i}^{(m_-)} + c_{t,i}'^\top p_{t,i}^{(m)} + \| \operatorname{diag}(c''_{t,i}) p_{t,i}^{(m)} \|_2^2. \tag{15}$$

Switching actions incur maintenance costs. This is accounted for by a term that is nonzero if units are enabled or disabled from node $m_- = \mathrm{anc}_i(m)$ to node m, i.e.,

$$\ell_{sw,i}^{(m)} = \| \operatorname{diag}(c_{sw,i})(\delta_{t,i}^{(m_-)} - \delta_{t,i}^{(m)}) \|_2^2, \tag{16}$$

with $c_{sw,i} \in \mathbb{R}_{>0}^{T_i}$ [11]. Here, $\delta_{t,i}^{(0)}$ equals the measured $\delta_{t,i}(k)$ at the current time instant k.

4) Control effort of lower layers: Large differences between power and setpoint can lead to additional control effort at the lower layers. Therefore, it is desirable to keep the power close to the setpoints. Since $\rho_i^{(m)}$ is correlated with deviations of the power from the setpoints, this desire can be reflected by a penalty, with weight $c_{\rho,i} \in \mathbb{R}_{>0}$, of the form

$$\ell_{\rho,i}^{(m)} = c_{\rho,i} \, (\rho_i^{(m)})^2. \tag{17}$$

5) Trading cost: All fluctuations are assumed to be covered locally inside each MG. As a result, p_g and consequently the cost for power exchange, i.e.,

$$\ell_{g,i}^{(m)} = c_{g,i} p_{g,i}(\mathrm{stage}_i(m)) + c'_{g,i} |p_{g,i}(\mathrm{stage}_i(m))| \tag{18}$$

with $c'_{g,i}$, $c''_{g,i} \in \mathbb{R}_{>0}$ [10], are certain. The first part of (18) represents a given price for energy and the second part a fixed cost per absolute value of traded energy.

6) Single MG cost: By construction of the scenario tree (see Section II-B.2), the expected cost is given by the sum over all nodes $m \in \mathbb{L}_i$, weighted with probability $\pi_i^{(m)}$, i.e.,

$$\ell_i = \sum_{m \in \mathbb{L}_i} \pi_i^{(m)} \big(\ell_{r,i}^{(m)} + \ell_{s,i}^{(m)} + \ell_{t,i}^{(m)} + \ell_{sw,i}^{(m)} + \ell_{\rho,i}^{(m)} + \ell_{g,i}^{(m)} \big) \gamma^{\mathrm{stage}_i(m)}. \tag{19}$$

Here, $\gamma \in (0,1)$ is used to emphasize near future decisions. Note that (19) equals the sum of expected stage costs over all $j \in \mathbb{N}_{[1,J]}$ in the scenario tree (see, e.g., [3, Ch. 10]).

B. Cost for power transmission

In addition to (19), costs for transmitting power are considered. Assuming that they increase with line losses, i.e., quadratically with the transmitted power p_e, allows us to deduce the transmission costs over prediction horizon J with diagonal matrix $C_e \in \mathbb{R}_{\geq 0}^{E \times E}$ as [10]

$$\ell_e = \sum_{j=1}^{J} p_e^\top(j) C_e p_e(j) \cdot \gamma^j. \tag{20}$$

C. MPC problem formulation

For each MG $i \in \mathbb{I}$, we collect all control inputs in $\mathbf{V}_i = [v_i^{(1)} \ \cdots \ v_i^{(M_i-1)}]$, states in $\mathbf{X}_i = [x_i^{(0)} \ \cdots \ x_i^{(M_i-1)}]$ and auxiliary variables in $\mathbf{Q}_i = [q_i^{(1)} \ \cdots \ q_i^{(M_i-1)}]$. Similarly, we form $\mathbf{P}_e = [p_e(1) \ \cdots \ p_e(J)]$ and $\mathbf{P}_g = [p_g(1) \ \cdots \ p_g(J)]$. Using these decision variables, we can formulate the following stochastic optimization problem.

Problem 1 (Central mixed-integer problem):

$$\begin{array}{l}\underset{\substack{\mathbf{V}_1,\dots,\mathbf{V}_I\\ \mathbf{X}_1,\dots,\mathbf{X}_I\\ \mathbf{Q}_1,\dots,\mathbf{Q}_I\\ \mathbf{P}_e,\mathbf{P}_g}}{\text{minimize}}\ \ell_e + \sum_{i\in\mathbb{I}} \ell_i \end{array}$$

subject to

(2) to (12) for all $m \in \mathbb{L}_i$
as well as initial conditions $x_i^{(0)} = x_i(k)$, $\delta_{t,i}^{(0)} = \delta_{t,i}(k)$
for all $i \in \mathbb{I}$. •

Remark 2 (Robustness): In Problem 1, power and energy, i.e., $\mathbf{X}_i$ and $\mathbf{Q}_i$, are monotone in the uncertain input [3, Remark 9.2.4]. Therefore, the formulation is stage-wise robust to uncertain inputs which are in the convex hull formed by $w_i^{(m)}$, $m \in \text{nodes}_i(j)$. In Section V, this property is exploited by adding extreme scenarios with low probabilities to the tree, which extends the convex hull and allow to increase robustness while keeping good performance when optimizing the expected cost. •

The decision variables $\delta_{t,i} \in \{0,1\}^{T_i}$ and $\delta_{r,i} \in \{0,1\}^{R_i}$ are Boolean, which renders Problem 1 a mixed-integer quadratic problem. In order to find a solution along the lines of [10], we relax $\delta_{t,i}^{(m)} \in [0,1]^{T_i}$ and $\delta_{r,i}^{(m)} \in [0,1]^{R_i}$, which allows to deduce the following quadratic formulation.

Problem 2 (Central relaxed problem):

$$\begin{array}{l}\underset{\substack{\mathbf{V}_1,\dots,\mathbf{V}_I\\ \mathbf{X}_1,\dots,\mathbf{X}_I\\ \mathbf{Q}_1,\dots,\mathbf{Q}_I\\ \mathbf{P}_e,\mathbf{P}_g}}{\text{minimize}}\ \ell_e + \sum_{i\in\mathbb{I}} \ell_i \end{array}$$

subject to

(2) to (12) for all $m \in \mathbb{L}_i$
as well as initial conditions $x_i^{(0)} = x_i(k)$, $\delta_{t,i}^{(0)} = \delta_{t,i}(k)$
with $\delta_{t,i}^{(m)} \in [0,1]^{T_i}$ and $\delta_{r,i}^{(m)} \in [0,1]^{R_i}$ for all $m \in \mathbb{L}_i$
and all $i \in \mathbb{I}$. •

IV. Distributed Solution

In this section, we describe how to find a (not necessarily optimal) distributed solution to Problem 1 using Algorithm 1. In detail, we first find a solution to Problem 2 by alternately solving a subproblem at a central coordinator and local subproblems at the MGs (see Figure 3). In a second step, local MIPs are solved at each MGs for the given PCC power from the previous step.

Consider a copy of $\mathbf{P}_g$ denoted $\hat{\mathbf{P}}_g = [\hat{p}_g(1) \ \cdots \ \hat{p}_g(J)]$. The decision variables in $\mathbf{P}_g$ are used at the local MGs and the ones in $\hat{\mathbf{P}}_g$ at the central entity. Both have to be found such that

$$\mathbf{P}_g - \hat{\mathbf{P}}_g = \mathbf{0}_{I\times J}\,. \tag{21}$$

Let us form the vector of Lagrange multipliers of all MGs at prediction step j as $\lambda(j) = [\lambda_1(j) \ \cdots \ \lambda_I(j)]^\top \in \mathbb{R}^I$ and collect them in $\mathbf{\Lambda} = [\lambda(1) \ \cdots \ \lambda(J)]$. We refer to row i of $\mathbf{\Lambda}$ as $\mathbf{\Lambda}_i$, to row i of $\mathbf{P}_g$ as $\mathbf{P}_{g,i}$ and to row i of $\hat{\mathbf{P}}_g$ as $\hat{\mathbf{P}}_{g,i}$. This allows us to formulate the augmented Lagrangian of Problem 2 with fixed parameter $\kappa \in \mathbb{R}_{>0}$,

$$\begin{aligned}\mathcal{L}_\kappa(\mathbf{P}_g, \hat{\mathbf{P}}_g, \mathbf{\Lambda}) = \ell_e + \sum_{i\in\mathbb{I}} \big(&\ell_i + \mathbf{\Lambda}_i(\mathbf{P}_{g,i} - \hat{\mathbf{P}}_{g,i})^\top \\ &+ \kappa/2 \|\mathbf{P}_{g,i} - \hat{\mathbf{P}}_{g,i}\|_2^2\big).\end{aligned} \tag{22}$$

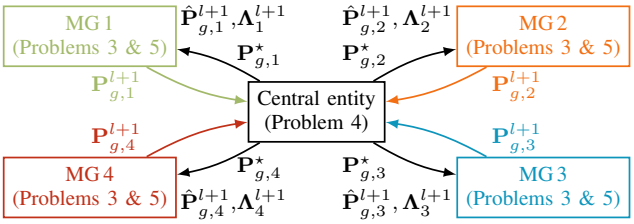

Fig. 3. Underlying communication structure in Algorithm 1.

Similar to [10], we intend to find a distributed solution to Problem 2 based on the augmented Lagrangian. Therefore, we pose the following optimization problems.

Problem 3 (Local ADMM problem at MG $i \in \mathbb{L}$):

$$\mathbf{P}_{g,i}^{l+1} \in \underset{\mathbf{V}_i,\mathbf{X}_i,\mathbf{Q}_i,\mathbf{P}_{g,i}}{\arg\min}\ \ell_i + \mathbf{\Lambda}_i^l \mathbf{P}_{g,i}^\top + \kappa/2 \|\mathbf{P}_{g,i} - \hat{\mathbf{P}}_{g,i}^l\|_2^2$$

subject to

(2) to (11) for all $m \in \mathbb{L}_i$
as well as initial conditions $x_i^{(0)} = x_i(k)$, $\delta_{t,i}^{(0)} = \delta_{t,i}(k)$
with $\delta_{t,i}^{(m)} \in [0,1]^{T_i}$, $\delta_{r,i}^{(m)} \in [0,1]^{R_i}$ for all $m \in \mathbb{L}_i$. •

Problem 4 (Central ADMM problem at coordinator):

$$\hat{\mathbf{P}}_g^{l+1} \in \underset{\hat{\mathbf{P}}_g,\mathbf{P}_e}{\arg\min}\ \ell_e - \sum_{i\in\mathbb{I}} \big(\mathbf{\Lambda}_i^l \hat{\mathbf{P}}_{g,i}^\top + \kappa/2 \|\mathbf{P}_{g,i}^{l+1} - \hat{\mathbf{P}}_{g,i}\|_2^2\big)$$

subject to

(10) and (12) using $\hat{p}_g(j)$ instead of $p_g(j)$
for all $j \in \mathbb{N}_{[1,J]}$. •

By alternately solving Problems 3 and 4 and updating Lagrange multipliers (see (23) in Algorithm 1) we can find an optimal solution to Problem 2 using the ADMM. The resulting optimal values $\mathbf{P}_{g,i}^\star$ are then used to find feasible (but not necessarily optimal) solutions to Problem 1 via local mixed-integer updates at all MGs. In these updates, $\mathbf{P}_g$ is fixed to $\mathbf{P}_{g,i}^\star$ and Boolean values for $\delta_{t,i}$ and $\delta_{r,i}$ are again considered. The associated problem reads as follows.

Problem 5 (Mixed-integer update at MG $i \in \mathbb{L}$):

$$\underset{\mathbf{V}_i,\mathbf{X}_i,\mathbf{Q}_i}{\text{minimize}}\ \ell_i$$

subject to

(2) to (9) and (11) for all $m \in \mathbb{L}_i$,
as well as initial conditions $x_i^{(0)} = x_i(k)$, $\delta_{t,i}^{(0)} = \delta_{t,i}(k)$
with fixed $\mathbf{P}_{g,i} = \mathbf{P}_{g,i}^\star$. •

Algorithm 1 allows us to find a hierarchical distributed solution using Problems 3 to 5 (see also Figure 3). Similar to [10], a termination criterion that checks if the change of Lagrange multipliers, PCC power, and residuals are all below a small $\epsilon \in \mathbb{R}_{>0}$. If this termination criterion is not met at $l = l_{\max}$, then $\hat{\mathbf{P}}_{g,i}^{l_{\max}+1}$, which represents a feasible solution to Problem 2, is used subsequently. Finally, in step 3, local MIPs are employed to find a feasible solution to Problem 1.

Remark 3 (Privacy): By design of Algorithm 1, the local MG controllers only share the PCC power forecast $\mathbf{P}_{g,i}^{l+1}$ with the central entity. Thus, no explicit information about the structure of the MG in the form of constraints or cost

function is shared with others which helps to preserve the privacy of the local MG controllers. One can, however, think of ways to reconstruct parts of Problem 3 using malicious vectors $\hat{\mathbf{P}}_{g,i}^{l+1}$, $\mathbf{\Lambda}_i^{l+1}$. Finding formulations which are secure against such attacks is subject to future work. •

Remark 4 (Suboptimality): The ADMM part of Algorithm 1 provides an optimal solution to Problem 2. However, the overall scheme, composed of ADMM and Problem 5 is not guaranteed to find an optimal solution to Problem 1. That being said, in the simulations performed in Section V, the algorithm was found to provide results with a small suboptimality gap to the original Problem 1. •

Remark 5 (Feasibility): Let us assume that each MG is configured such that storage and conventional units together can always serve all possible load values present in the forecast scenarios. Thus, an islanded operation where all RESs are set to provide zero power always represents a feasible solution to Problem 5. This allows us to deal with ADMM solutions $\mathbf{P}_{g,i}^{\star}$ which lead to infeasible formulations of Problem 5 at MG i by re-executing Algorithm 1 with zero PCC power using $p_{g,i}^{\min} = p_{g,i}^{\max} = 0$. This results in $\mathbf{P}_{g,i}^{\star} = \mathbf{0}_{1\times J}$ which in turn lead to feasible formulations of Problem 5. Another alternative is to employ schemes that ensure feasibility, such as the one presented in [21]. For a thorough discussion of feasibility in a related problem, the reader is kindly referred to [10, Sec. V.C]. •

Algorithm 1 Hierarchical distributed algorithm

1. **Initialize:** At time k, $\forall i \in \mathbb{I}$, measure $x_i(k)$, $\delta_{t,i}(k)$ and obtain scenario tree.
2. **ADMM loop:**
   for $l = 0, \ldots, l_{\max} \in \mathbb{N}$:
   (i) For all MG $i \in \mathbb{I}$ (in parallel):
   - Solve Problem 3 in parallel to obtain $\mathbf{P}_{g,i}^{l+1}$.
   - Send $\mathbf{P}_{g,i}^{l+1}$ to central entity.

   (ii) Central entity:
   - Solve Problem 4 to obtain $\hat{\mathbf{P}}_{g}^{l+1}$.
   - Update Lagrange multipliers:

$$\mathbf{\Lambda}^{l+1} = \mathbf{\Lambda}^{l} + \kappa\big(\mathbf{P}_{g}^{l+1} - \hat{\mathbf{P}}_{g}^{l+1}\big). \tag{23}$$

   - Communicate $\hat{\mathbf{P}}_{g,i}^{l+1}$ and $\mathbf{\Lambda}_i^{l+1}$ to all MG $i \in \mathbb{I}$.
   - Check termination criterion:
     if $\big(|\mathbf{\Lambda}^{l} - \mathbf{\Lambda}^{l+1}| < \epsilon$ and $|\mathbf{P}_{g,i}^{l} - \mathbf{P}_{g,i}^{l+1}| < \epsilon$ and $|\mathbf{P}_{g,i}^{l+1} - \hat{\mathbf{P}}_{g,i}^{l+1}| < \epsilon\big)$ or $l = l_{\max}$,
     then set $\mathbf{P}_{g,i}^{\star} = \hat{\mathbf{P}}_{g,i}^{l+1}$ and go to 3.
3. **Mixed-integer update:** For all MG $i \in \mathbb{I}$ (in parallel):
   - Solve Problem 5.

Algorithm 1 represents the core of an MPC scheme: At each time instant k, new scenario trees and new measurements $x_i(k)$, $\delta_{t,i}(k)$ are obtained at each MG $i \in \mathbb{I}$. Then, Algorithm 1 is used to find control actions $v_i^{(1)}$ which are applied to the each MG $i \in \mathbb{I}$. At time $k+1$, new measurements and new scenario trees are obtained and the scheme is repeated in a receding horizon manner.

TABLE II
SIMULATION PARAMETERS ($i = 1, \ldots, 4$)

Parameter	Value	Parameter	Value
$[x_i^{\min},\ x_i^{\max}]$	$[0.2,\ 6]\,\mathrm{puh}$	$[p_{\mathrm{e},i}^{\min},\ p_{\mathrm{e},i}^{\max}]$	$[-1,\ 1]\,\mathrm{pu}$
$[p_{t,i}^{\min},\ p_{t,i}^{\max}]$	$[0.4,\ 1]\,\mathrm{pu}$	$[p_{g,i}^{\min},\ p_{g,i}^{\max}]$	$[-1,\ 1]\,\mathrm{pu}$
$[p_{s,i}^{\min},\ p_{s,i}^{\max}]$	$[-1,\ 1]\,\mathrm{pu}$	$K_{s,i} = K_{t,i}$	1
$[p_{r,i}^{\min},\ p_{r,i}^{\max}]$	$[0,\ 2]\,\mathrm{pu}$	$[\delta_1(0), \ldots, \delta_4(0)]$	[0, 0, 0, 0]

TABLE III
WEIGHTS IN COST FUNCTIONS OF ALL MGS ($i = 1, \ldots, 4$).

Weight	Value	Weight	Value
$c_{r,i}$	$1\ {}^{1}/_{\mathrm{pu}}$	$c_{sw,i}$	0.1
$c_{s,i}$	$0.2236\ {}^{1}/_{\mathrm{pu}}$	$c_{g,i}$	$0.5\ {}^{1}/_{\mathrm{pu}}$
$c_{t,i}$	0.1178	$c'_{g,i}$	$0.1\ {}^{1}/_{\mathrm{pu}}$
$c'_{t,i}$	$0.751\ {}^{1}/_{\mathrm{pu}}$	C_{e}	$0.1 \cdot \mathrm{diag}([1,2,3,6]^{\top})\,{}^{1}/_{\mathrm{pu}^2}$
$c''_{t,i}$	$0.0693\ {}^{1}/_{\mathrm{pu}}$	$c_{\sigma,i}$	1000
$c_{\rho,i}$	0.05	γ	0.95

V. CASE STUDY

The following study compares the closed-loop results obtained with Algorithm 1 with those of the certainty equivalence approach from [10]. We start with the simulation setup.

A. Simulation setup

In what follows, the network in Figure 1 with the simulation parameters in Table II is considered. As initial state, $[x_1(0), \ldots, x_1(0)] = [1, 3.4, 2.9, 5.6]\,\mathrm{puh}$ and as line admittances $y_{e,i} = 20\,\mathrm{pu}$, $i \in \mathbb{N}_{[1,4|}$ were used. Additionally, the weights in Table III were employed in the cost functions.

The simulation was executed for 336 steps with a sampling interval of $30\,\mathrm{min}$., resulting in a total duration of 7 days. In the MPC schemes, a forecast prediction horizon of 12 sampling intervals was considered. The four scenario trees, i.e., one for each MG to formulate Problems 3 and 5, were generated from 500 independent forecast scenarios at each execution of the controller. These scenarios were deduced from Monte-Carlo simulations assuming wind speed, irradiance and demand forecasts with normally distributed residuals. A branching factor of 6 at stage 1, 2 at stage 2 and 1 for all subsequent stages was considered. Each tree was generated using forward selection [14]. To each tree the largest and smallest forecast (at the first prediction step) from the collections of independent scenarios were added to increase robustness (see [3, Section 12.1.2]).

Closed-loop simulations with three distributed approaches were performed: (i) *Certainty equivalence MPC*: This state-of-the-art approach is based on [10, Algorithm 1]. The uncertain input is assumed to be given by the nominal forecast. Note that for comparability, switching costs were added to the approach from [10]. (ii) *Stochastic MPC*: This approach is based on Algorithm 1. It employs forecasts in the form of scenario trees. (iii) *Prescient MPC*: This approach is used as a reference and based on [10, Algorithm 1]. Here, a hypothetical perfect forecast, given by the actual measured

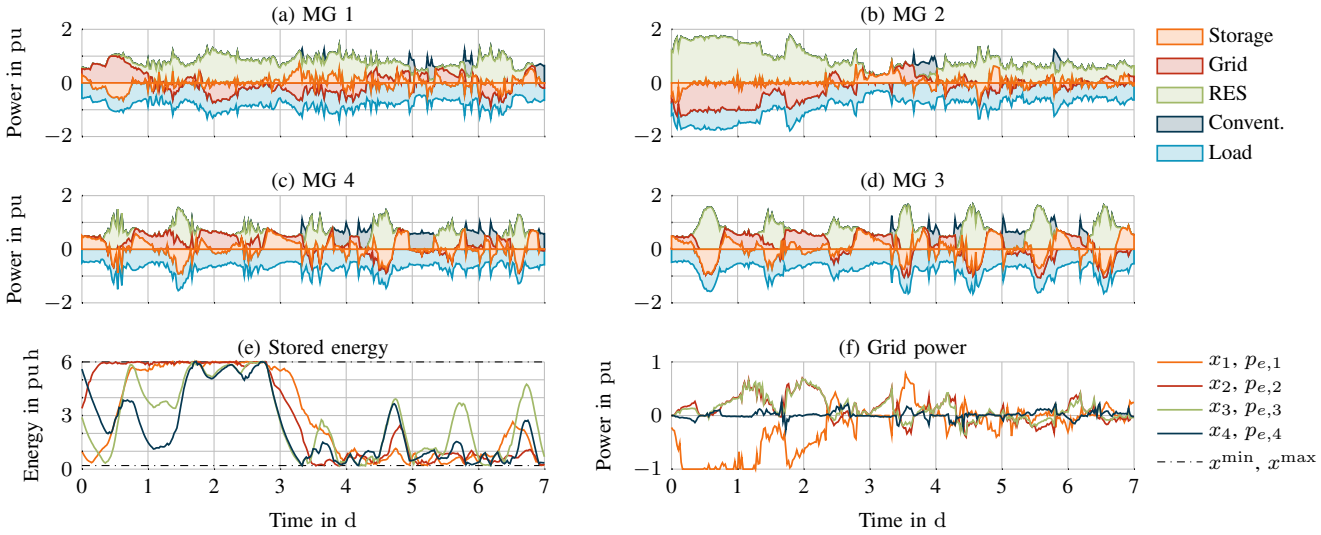

Fig. 4. Closed-loop simulation results obtained with Algorithm 1.

future load and available renewable infeed, is employed. The setpoints found through them are passed to a model of the network of interconnected MGs which simulates the system behavior. The case study was implemented in MATLAB R2020b using YALMIP (R20201001) [22] and Gurobi 9.1.0 as numerical solver.

B. Closed-loop simulations

Figure 4 shows power and energy when using Algorithm 1. The photovoltaic generators of MGs 3 and 4 come with a daily seasonality. This is also reflected in power and energy of the storage units in these MGs. Moreover, the power line between MGs 3 and 4 is hardly utilized, because of similar renewable infeed and load patterns. The power provided by the wind turbines in MGs 1 and 2 does not come with notable seasonality. MG 2 exhibits a high renewable share on the first two days which is partly traded with other MGs. From day 3 on, the available renewable infeed decreases. Up to this time, all demand could be met without conventional generation. After day 3, conventional units need to switch on at times to meet the demand. However, their infeed remains small compared to RESs.

1) Violation of operating bounds: The storage units' soft bounds $x_i^{\min} = 0.2\,\mathrm{pu\,h}$ and $x_i^{\max} = 6\,\mathrm{pu\,h}$ for $i \in \mathbb{N}_{[1,4]}$ mark a desired range of operation. Figure 5 shows a comparison with respect to this aspect. We can see that the stochastic MPC causes a smaller number of less extreme values outside of the desired interval compared to certainty equivalence MPC. Moreover, violations of power limits could only be observed with the certainty equivalence MPC. In total, 52 power limit violations (mean value: $0.012\,\mathrm{pu}$, maximum: $0.063\,\mathrm{pu}$) occurred. Unlike the desired range of energy, these violations seriously jeopardize a safe operation. The stochastic MPC did not cause any power limit violation, which hints at improved safety when using Algorithm 1.

2) Closed-loop performance: Table IV contains the total generation of renewable and conventional units over the simulation horizon. Moreover, accumulated closed-loop operating costs of all MGs, transmission costs and overall costs are summarized. As expected, the prescient controller achieves the best results. The certainty equivalence MPC yields the worst costs and the stochastic MPC takes the middle position. Compared to the certainty equivalence case, renewable infeed of the stochastic approach is much higher and comes very close to the prescient case. Moreover, the stochastic MPC could reduce the share of conventional energy compared to the certainty equivalence MPC by 25.9 %, the number of switching actions by 13 % and the overall cost by 40 %.

C. Computational properties

1) Solve times: In what follows, we will discuss the accumulated solve times for each simulation step, i.e., each execution of Algorithm 1 and [10, Algorithm 1]. The simulations were executed on a computer with an Intel®Xeon®E5-1620 v2 processor @3.70 GHz with 32 GB RAM. The certainty equivalence and the prescient MPC yield very similar solve times (mean: 1 s, maximum: 11 s). The stochastic MPC requires a multiple of this (mean: 9 s, maximum:

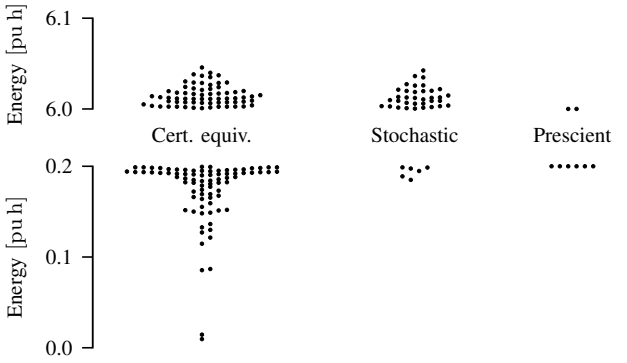

Fig. 5. Energy values outside of desired range. Motivated by the precision of the numerical solver, values closer than 10^{-5} to the interval were omitted.

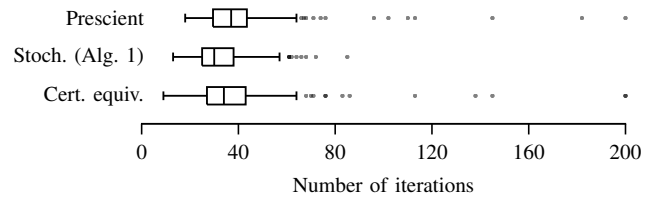

Fig. 6. Boxplots of number of ADMM iterations for different approaches.

223 s), which is noncritical considering a sampling interval of 30 min.. Compared to Problem 1 (mean: 127 s), the solve times of Algorithm 1 are significantly reduced and only come at the cost of a small suboptimality gap (mean: 0.3 %).

2) ADMM convergence: Figure 6 shows boxplots that illustrate the number of iterations required by the different algorithms when considering a tolerance of $\epsilon = 10^{-4}$ and $l_{\max} = 200$. We can see that the median of all cases is below 40. Algorithm 1 comes with the lowest median which is as little as 30 iterations and a maximum of 85 iterations. A deeper look into the simulation reveals that outliers with a very high number of iterations seem to occur when all four MGs have similar conditions, i.e., either a surplus of RESs and full storage units or empty storage units and little available renewable infeed. However, for a sampling time 30 min., 200 iterations at maximum appear tolerable.

VI. Conclusions

In this work, a scenario-based stochastic MPC scheme for the operation of interconnected MGs was presented. Based on a central MPC formulation, a distributed algorithm that employs the ADMM was developed. The algorithm reflects the hierarchical structure in the network of interconnected MG: local controllers are in charge of individual MGs, while a central entity is in charge of the transmission grid. In closed-loop simulations, the novel approach outperformed the certainty equivalence one concerning the number of constraint violations and the costs. Moreover, the algorithm converges sufficiently fast for operation control.

Future work concerns simulations with a larger number of MGs and theoretical analyses concerning the scalability of the approach. Moreover, suboptimality, persistent feasibility and privacy shall be further investigated.

TABLE IV
Accumulated closed-loop simulation results

		Certainty equival.	Stochastic (Alg. 1)	Prescient
Renewable energy in pu h		318.1	333.8	334.0
Conventional energy in pu h		61.0	45.2	45.9
No. of switching actions		46	40	29
Costs	MG 1	1 652.8	1 005.9	786.8
	MG 2	1 366.1	774.2	607.7
	MG 3	2 000.2	1086.1	1 003.8
	MG 4	1 755.3	1154.3	1 109.9
	Transmission	21.7	19.0	18.7
	Sum	6 796.1	4 039.5	3 527.0

References

[1] D. E. Olivares, A. Mehrizi-Sani, A. H. Etemadi, C. A. Cañizares, R. Iravani, M. Kazerani, A. H. Hajimiragha, O. Gomis-Bellmunt, M. Saeedifard, R. Palma-Behnke, G. A. Jiménez-Estévez, and N. D. Hatziargyriou, "Trends in microgrid control," *IEEE Trans. Smart Grid*, vol. 5, no. 4, pp. 1905–1919, 2014.

[2] P. Piagi and R. Lasseter, "Autonomous control of microgrids," in *IEEE PES General Meeting*, 2006.

[3] C. A. Hans, *Operation control of islanded microgrids*. Shaker Verlag, 2021.

[4] S. Mohammadi, S. Soleymani, and B. Mozafari, "Scenario-based stochastic operation management of microgrid including wind, photovoltaic, micro-turbine, fuel cell and energy storage devices," *Int. J. Electr. Power Energy Syst.*, vol. 54, pp. 525–535, 2014.

[5] P. Kou, D. Liang, and L. Gao, "Stochastic energy scheduling in microgrids considering the uncertainties in both supply and demand," *IEEE Syst. J.*, vol. 12, no. 3, pp. 2589–2600, 2018.

[6] M. Petrollese, L. Valverde, D. Cocco, G. Cau, and J. Guerra, "Real-time integration of optimal generation scheduling with MPC for the energy management of a renewable hydrogen-based microgrid," *Appl. Energy*, vol. 166, pp. 96–106, 2016.

[7] A. Maulik and D. Das, "Optimal operation of droop-controlled islanded microgrids," *IEEE Trans. Sustainable Energy*, vol. 9, no. 3, pp. 1337–1348, 2017.

[8] B. Heymann, J. F. Bonnans, F. Silva, and G. Jimenez, "A stochastic continuous time model for microgrid energy management," in *ECC*, 2016, pp. 2084–2089.

[9] N. Bazmohammadi, A. Tahsiri, A. Anvari-Moghaddam, and J. M. Guerrero, "A hierarchical energy management strategy for interconnected microgrids considering uncertainty," *Int. J. Electr. Power Energy Syst.*, vol. 109, pp. 597–608, 2019.

[10] C. A. Hans, P. Braun, J. Raisch, L. Grüne, and C. Reincke-Collon, "Hierarchical distributed model predictive control of interconnected microgrids," *IEEE Trans. Sustainable Energy*, vol. 10, no. 1, pp. 407–416, 2019.

[11] C. A. Hans, P. Sopasakis, A. Bemporad, J. Raisch, and C. Reincke-Collon, "Scenario-based model predictive operation control of islanded microgrids," in *54th IEEE CDC*, 2015, pp. 3272–3277.

[12] A. La Bella, M. Farina, C. Sandroni, and R. Scattolini, "Design of aggregators for the day-ahead management of microgrids providing active and reactive power services," *IEEE Trans. Control Syst. Technol.*, vol. 28, no. 6, pp. 2616–2624, 2020.

[13] F. Rey, X. Zhang, S. Merkli, V. Agliati, M. Kamgarpour, and J. Lygeros, "Strengthening the group: Aggregated frequency reserve bidding with ADMM," *IEEE Trans. Smart Grid*, vol. 10, no. 4, pp. 3860–3869, 2019.

[14] H. Heitsch and W. Römisch, "Scenario reduction algorithms in stochastic programming," *Comput. Optim. Appl.*, vol. 24, no. 2-3, pp. 187–206, 2003.

[15] T. Ding, Y. Hu, and Z. Bie, "Multi-stage stochastic programming with nonanticipativity constraints for expansion of combined power and natural gas systems," *IEEE Trans. Power Syst.*, vol. 33, no. 1, pp. 317–328, 2018.

[16] A. Shapiro, D. Dentcheva, and A. Ruszczyński, *Lectures on stochastic programming: modeling and theory*, 2nd ed. SIAM, 2014.

[17] R. T. Rockafellar and R. J.-B. Wets, "Nonanticipativity and $\mathcal{L}^1$-martingales in stochastic optimization problems," in *Stochastic Systems: Modeling, Identification and Optimization, II*. Springer, 1976, pp. 170–187.

[18] J. Schiffer, C. A. Hans, T. Kral, R. Ortega, and J. Raisch, "Modelling, analysis and experimental validation of clock drift effects in low-inertia power systems," *IEEE Trans. Ind. Electron.*, vol. 64, no. 7, pp. 5942–5951, 2017.

[19] K. Purchala, L. Meeus, D. Van Dommelen, and R. Belmans, "Usefulness of DC power flow for active power flow analysis," in *IEEE PES General Meeting*, 2005, pp. 454–459.

[20] M. Živić Đurović, A. Milačić, and M. Kršulja, "A simplified model of quadratic cost function for thermal generators," *Ann. DAAAM 2012 Proc. 23 Int. DAAAM Symp.*, vol. 23, no. 1, pp. 25–28, 2012.

[21] A. K. Sampathirao, S. Hofmann, J. Raisch, and C. A. Hans, "Distributed conditional cooperation model predictive control of interconnected microgrids," *Automatica*, vol. 157, p. 111258, 2023.

[22] J. Löfberg, "YALMIP: A toolbox for modeling and optimization in MATLAB," in *IEEE CACSD*, 2004, pp. 284–289.